

1  
2  
3

# JAST (Journal of Animal Science and Technology) TITLE PAGE

Upload this completed form to website with submission

ARTICLE INFORMATION	Fill in information in each box below
Article Type	Research article
Article Title (within 20 words without abbreviations)	Characteristics between porcine bone marrow-derived mesenchymal stem and peripheral blood mononuclear cells
Running Title (within 10 words)	Porcine bone marrow-derived mesenchymal stem characteristics
Author	Young Kyu Kim <sup>1,4</sup> , Ju Young Lee <sup>1,4</sup> , Ji Woo Shin <sup>1,2</sup> , Jeong Ho Hwang <sup>1,3,*</sup>
Affiliation	<p><sup>1</sup>Center for Large Animals Convergence Research, Korea Institute of Toxicology, 30 Baekhak 1 Gil, Jeongeup-Si, Jeonbuk-Do, 56212, Republic of Korea</p> <p><sup>2</sup>Laboratory Animal Medicine, College of Veterinary Medicine, Chungnam National University, Daejeon 34134, Republic of Korea</p> <p><sup>3</sup>Companion Animal New Drug Development Center, Korea Institute of Toxicology, 30 Baekhak1-Gil, 56212 Jeongeup-Si, Jeonbuk-Do, Republic of Korea</p> <p><sup>4</sup>These authors contributed equally.</p>
ORCID (for more information, please visit <a href="https://orcid.org">https://orcid.org</a> )	<p><a href="https://orcid.org/0000-0001-7503-2945">https://orcid.org/0000-0001-7503-2945</a>,</p> <p><a href="https://orcid.org/0000-0002-5375-4688">https://orcid.org/0000-0002-5375-4688</a>,</p> <p><a href="https://orcid.org/0009-0008-1370-576X">https://orcid.org/0009-0008-1370-576X</a>,</p> <p><a href="https://orcid.org/0000-0002-4763-8373">https://orcid.org/0000-0002-4763-8373</a></p>
Competing interests	No potential conflict of interest relevant to this article was reported.
Funding sources State funding sources (grants, funding sources, equipment, and supplies). Include name and number of grant if available.	Korea institute of Toxicology (KIT, Korea) and the Ministry of Science and ICT (grant numbers KK-2408-01, 1711195889).
Acknowledgements	The author(s) disclosed receipt of the following financial support for the research, authorship, and/or publication of this article: This work

	was supported by grants from the Korea Institute of Toxicology (KIT, Korea) and the Ministry of Science and ICT (grant numbers KK-2408-01, 1711195889).
<b>Availability of data and material</b>	Upon reasonable request, the datasets of this study can be available from the corresponding author.
<b>Authors' contributions</b> Please specify the authors' role using this form.	Conceptualization: Hwang J Data curation: Kim Y, Lee J Formal analysis: Kim Y, Lee J, Shin J Methodology: Kim Y, Lee J, Shin J Software: Kim Y, Lee J, Shin J Validation: Kim Y, Lee J, Shin J, Hwang J Investigation: Kim Y, Lee J, Shin J Writing - original draft: Kim Y Writing - review & editing: Kim Y, Lee J, Shin J, Hwang J
<b>Ethics approval and consent to participate</b>	This article does not require IRB/IACUC approval because there are no human and animal participants.

4

## 5 CORRESPONDING AUTHOR CONTACT INFORMATION

<b>For the corresponding author (responsible for correspondence, proofreading, and reprints)</b>	<b>Fill in information in each box below</b>
First name, middle initial, last name	Jeong Ho, Hwang,
Email address – this is where your proofs will be sent	jeongho.hwang@kitox.re.kr
Secondary Email address	Hjh5847@gmail.com
Address	Animal Model Research Group, Korea Institute of Toxicology, 30, Baekhak 1-gil, Jeongeup-si, Jeollabuk-do 56212, Korea
Cell phone number	+82-10-2036-3722
Office phone number	+82-63-570-8528
Fax number	+82-63-570-8999

6

7

8  
9  
10  
11  
12  
13  
14  
15  
16  
17  
18  
19  
20  
21  
22  
23  
24  
25  
26  
27  
28  
29

## Abstract

Mesenchymal stem cells (MSCs) have been isolated from various organs and extensively studied for their potential in regulating transplantation. MSCs from different mammalian species are well characterized; however, the properties and therapeutic potential of porcine bone marrow-derived MSCs (BM-MSCs) remain unclear. In this study, we aimed to profile the characteristics of porcine BM-MSCs by comparing their gene expression patterns and immunomodulatory properties with those of porcine peripheral blood mononuclear cells (PBMCs) and bone marrow-attached cells (BMACs). Using quantitative polymerase chain reaction, flow cytometry, immunocytochemistry, and RNA sequencing, we confirmed the expression of key MSC markers, including CD105, CD73, and CD90, in porcine BM-MSCs, and aligned them closely with human MSCs. We found significant differences in gene expression between BM-MSCs and PBMCs, with BM-MSCs exhibiting a distinct expression pattern similar to that of BMACs. Gene ontology enrichment analysis revealed the pathways involved in immune modulation and tissue repair, underscoring the potential of BM-MSCs to enhance immune regulation. Notably, BM-MSCs exhibited higher transforming growth factor-beta levels than PBMCs, suggesting a central role in their immunosuppressive function. These findings indicate the immunomodulatory capabilities of porcine BM-MSCs and support their application in xenotransplantation, where they may help mitigate graft rejection and promote tissue regeneration.

**Keywords:** Porcine BM-MSC, PBMC, BMAC, TGF- $\beta$ , Xenotransplantation.

## INTRODUCTION

30

31 Mesenchymal stem cells (MSCs) are multipotent stromal cells recognized in regenerative medicine  
32 and transplantation for their potential to differentiate into various cell types and modulate immune  
33 responses (1-3). They have been widely studied in several species, particularly humans and they  
34 have shown therapeutic potential to treat various conditions such as cardiovascular diseases,  
35 neurodegenerative disorders, and immune-mediated diseases (4, 5). In addition to humans, studies  
36 have also been conducted on the characteristics of MSCs from various animal species, including  
37 dogs, goats, pigs, rabbits, and sheep, which generally exhibit positive CD44 expression and  
38 negative CD45 expression (6-9). Furthermore, recent reports highlight the application of MSCs in  
39 treating conditions such as musculoskeletal diseases, skin disorders, ocular diseases,  
40 neuromuscular disorders, chronic gingivitis, inflammatory bowel disease, and asthma in  
41 companion animals (10-12). However, the biological characteristics and potential applications of  
42 porcine MSCs remain unclear and require further investigation (5). Pigs are known to share  
43 significant similarities with humans in physical, biochemical, anatomical, and gene expression  
44 patterns, making them valuable as preclinical trial animals (13-15). Moreover, the high functional  
45 and anatomical similarity of the heart and kidney to those of humans has led to the recent use of  
46 pigs as a means for xenotransplantation (16-19). Consequently, porcine MSCs are particularly  
47 valuable for preclinical research and therapeutic applications, including their role in  
48 xenotransplantation (20).

49 The application of porcine bone marrow (BM)-derived MSCs (BM-MSCs) is promising in  
50 veterinary medicine and as a model for studying disease mechanisms and developing therapeutic  
51 strategies in translational research (21). Their immunomodulatory properties suggest that they may  
52 be crucial to reducing immune responses associated with graft rejection, making them a promising  
53 tool for improving the success of organ and tissue transplantation (22-25). Notably, their ability to

54 promote tissue repair and reduce inflammation has been reported in recent studies, reinforcing  
55 their potential use in regenerative medicine (26-29).

56 MSCs are typically identified by specific surface markers critical for their immunomodulatory  
57 functions, such as CD73, CD90, and CD105; however, they lack hematopoietic markers, such as  
58 CD45 (6, 21, 30). These markers have been extensively used to characterize MSCs across different  
59 species, providing a basis for their identification and therapeutic applications (31, 32). Despite the  
60 recognized importance of these markers, limited data exist on the expression profiles and  
61 functional characteristics of porcine BM-MSCs (33). A comprehensive understanding of these  
62 characteristics is crucial for developing effective MSC-based therapies and enhancing  
63 transplantation success (34, 35).

64 In the present study, we aimed to profile the characteristics of porcine BM-MSCs by comparing  
65 their expression patterns with those of porcine peripheral blood mononuclear cells (PBMCs), BM-  
66 attached cells (BMACs), and the porcine kidney epithelial cell line (PK(15)). BMACs and PBMCs  
67 were chosen as comparators because they represent distinct populations within the bone marrow  
68 and peripheral blood compartments. BMACs, which include stromal cells, macrophages, and other  
69 bone marrow-derived cells, support stem cell function (36, 37), while PBMCs are peripheral  
70 immune cells used to understand the immunomodulatory properties of BM-MSCs (38, 39). This  
71 comparison highlights the regulatory mechanisms of BM-MSCs and provides insights into their  
72 therapeutic potential in regenerative medicine and transplantation. Using quantitative real-time  
73 polymerase chain reaction (qRT-PCR), flow cytometry, immunocytochemistry, and RNA  
74 sequencing, we aimed to elucidate the molecular and phenotypic features that distinguish BM-  
75 MSCs from other cell types. This study focused on the immunomodulatory functions and potential  
76 applications of BM-MSCs in mitigating graft rejection and promoting tissue regeneration.

77

## MATERIALS AND METHODS

78

### 79 **Cells**

80 Porcine BM-MSCs (Cell Biologics, IL, USA), purchased from Cell Biologics and isolated from  
81 porcine tibias and femurs, were cultured in mesenchymal cell medium (Cell Biologics) containing  
82 10% heat-inactivated fetal bovine serum (FBS, Gibco, MA, USA) and 1% penicillin/streptomycin  
83 (P/S, Cell Biologics) at 37 °C in an incubator with a 5% carbon dioxide (CO<sub>2</sub>) atmosphere. Porcine  
84 BM cells were isolated from the humerus, tibia, and femurs of stillborn piglets. After a 10-d culture  
85 period in a culture dish, non-adherent cells were removed by discarding the supernatant. The  
86 remaining adherent cells were cultured and indicated as BMACs. BMACs and PK(15) (American  
87 Type Culture Collection, VA, USA) cells were maintained in Dulbecco's Modified Eagle's  
88 Medium (DMEM, Gibco) containing 10% FBS, 1% minimum essential medium non-essential  
89 amino acid solution, and 1% P/S at 37 °C in an incubator with a 5% CO<sub>2</sub> atmosphere.

90 THP-1 cell line (Korean Cell Line Bank, Seoul, South Korea) was cultured in Roswell Park  
91 Memorial Institute 1640 medium (RPMI 1650, Gibco) containing 10% FBS and 1% P/S (Gibco)  
92 at 37 °C in an incubator with a 5% CO<sub>2</sub> atmosphere. To obtain phorbol-12-myristate-13-acetate  
93 (PMA)-differentiated THP-1 cells, THP-1 cells were differentiated using 10 ng/mL PMA (Sigma,  
94 MA, USA), and the PMA-free medium was changed the next day for 24 h. No contamination was  
95 detected in any cell cultures.

96

### 97 **Isolation of messenger RNA and RT-PCR**

98 Total RNA was isolated using Trizol (Life Technologies, CA, USA). Total cellular RNA was used  
99 to synthesize complementary DNA (cDNA) using a QuantiTect Reverse Transcription Kit (Qiagen,  
100 Hilden, Germany) according to the manufacturer's instructions.

101

## 102 **qRT-PCR**

103 Quantitative PCR (qPCR, Power SYBR™ Green PCR Master Mix, 4368702, Applied  
104 Biosystems, CA, USA) was performed using porcine primers for glyceraldehyde-3-phosphate  
105 dehydrogenase (GAPDH), CD73, CD90, and CD105 and human primers for GAPDH, tumor  
106 necrosis factor-alpha (TNF $\alpha$ ), interleukin (IL)-6, IL-10, C-C chemokine receptor type 7 (CCR7),  
107 and CD163. All qPCR primers were designed using Primer 3V0.4.0 (Table 1). qPCR was  
108 performed as follows: 95 °C for 10 min, 40 cycles at 95 °C for 15 s, and 60 °C for 1 min on a PCR  
109 machine (A28134, Applied Biosystems). Messenger RNA (mRNA) levels were determined using  
110 GAPDH ( $\Delta\text{Ct}=\text{Ct gene of interest} - \text{Ct GAPDH}$ ) and reported as relative mRNA expression ( $\Delta$   
111  $\Delta\text{Ct}=2^{\Delta\text{Ct sample}-\Delta\text{Ct control}}$ ) or the fold change.

## 112 **Flow cytometry**

113 Cells in each group were collected in fluorescence-activated cell sorting tubes (BD, NJ, USA) and  
114 washed twice with ice-cold phosphate-buffered saline (PBS). BM-MSCs and PBMCs were stained  
115 with allophycocyanin (APC)-conjugated CD44 (Abcam, Cambridge, UK), CD45 (Bio-Rad, CA,  
116 USA), CD73 (Invitrogen, MA, USA), CD90 (Abcam), and CD105 (Invitrogen) for 1 h at room  
117 temperature. Alexa Fluor 488-conjugated goat anti-mouse immunoglobulin (Ig) G (Invitrogen),  
118 488-conjugated donkey anti-sheep IgG (Invitrogen), and 568-conjugated goat anti-mouse IgG  
119 (Invitrogen) were used for cell labeling. Stained cells were analyzed using flow cytometry  
120 (Beckman Coulter, CA, USA) and CytExpert software (Beckman Coulter). For each sample, a cell  
121 count of 5,000 cells was obtained. The region of each sample was selected for the forward and side  
122 scatters, and a histogram was used to measure the mean fluorescence intensity of fluorescein  
123 isothiocyanate, phycoerythrin, or APC.

124

## 125 **Immunocytochemistry**

126 After fixation in 4% paraformaldehyde in Dulbecco's PBS, the cells were stained with CD45 (Bio-  
127 Rad, MCA1222GA), CD73 (Invitrogen), and CD105 (Invitrogen). Alexa Fluor 647-conjugated  
128 goat anti-mouse IgG (Invitrogen) and 488-conjugated donkey anti-sheep IgG (Invitrogen) were  
129 used for cell labeling. Nuclei were stained with a mounting medium containing 4',6-diamidino-2-  
130 phenylindole (Abcam). A confocal microscope (ZEISS, Baden-Württemberg, Germany) was used  
131 to obtain images.

132

## 133 **mRNA sequencing**

134 Notably, 1 µg RNA was isolated from  $3 \times 10^6$  cells using the phenol/chloroform extraction method.  
135 RNA integrity was assessed using an Agilent 2100 Bioanalyzer (Agilent, CA, USA). Each cDNA  
136 library was prepared using a QuantSeq 3mRNA-seq Library Prep Kit (Lexogen, Vienna, Austria).  
137 The entire process, including sequencing, mapping, and normalization, was performed according  
138 to the manufacturer's instructions. Differentially expressed genes (DEGs) were determined from  
139 the genes with expression levels changed as  $|\log_2(\text{fold change})| \geq 2$ . Excel-based DEG Analysis  
140 (ExDEGA; E-biogen, Inc., Seoul, South Korea) was used to visualize the hierarchical heatmap and  
141 create a Venn diagram of DEGs.

142

## 143 **GO analysis**

144 To compare functional annotations among BM-MSCs, BMACs, and PBMCs, Kyoto Encyclopedia  
145 of Genes and Genomes pathway analysis was performed using the Database for Annotation,  
146 Visualization, and Integrated Discovery Bioinformatics Resources 6.8 (40, 41). Furthermore,  
147 upstream regulators, such as the main biological network, canonical pathway, and upstream  
148 regulator identification, were analyzed using IPA (Qiagen, CA, USA).



149

### 150 **Indirect co-culture system**

151 PMA-differentiated THP-1 cells were treated with 1 µg/mL lipopolysaccharide (LPS; Sigma,  
152 LPS25) for 24 h and seeded in a 12-well plate (Greiner, 665180) at a density of  $1 \times 10^6$  cells/well.  
153 The same number of BM-MSCs was seeded in Transwell inserts (Greiner, 665640). After 24 h,  
154 PMA-differentiated THP-1 cells in the bottom plate were evaluated for IL-1 $\beta$ , IL-6, TNF $\alpha$ , IL-10,  
155 CCR7, and CD163 mRNA expression using qRT-PCR.

156

### 157 **Statistical analysis**

158 All data are presented as the mean  $\pm$  standard deviation. All experiments were performed at least  
159 thrice. Statistical significance was determined using Student's t-test (two-tailed) or analysis of  
160 variance using GraphPad Prism 8 software (GraphPad, Inc., La Jolla, CA, USA). The *p*-value and  
161 Z-score were calculated using the computational algorithms of Student's t-test and Fisher's exact  
162 test to confirm statistical significance.

163

## 164 **RESULTS**

### 165 **Characterization of Porcine BM-MSCs compared to BMAC and PBMC**

166 To characterize porcine BM-MSCs, BM-MSCs obtained from Cell Biologics were compared with  
167 porcine PBMCs, BMACs, and PK(15) cells to analyze the expression patterns of BM-MSC  
168 markers. Previous studies have reported that MSCs can be identified and characterized based on  
169 the expression of specific surface markers. First, we analyzed the mRNA expression patterns of  
170 CD105, CD73, and CD90, which are human MSC markers, in BM-MSCs, PBMCs, and BMACs  
171 and compared them to those in PK(15) cells using qRT-PCR. The mRNA expression levels of  
172 CD73, CD90, and CD105 were confirmed in BM-MSCs and BMACs and exhibited an expression

173 pattern consistent with that observed in human MSCs (Figure 1A). Using flow cytometry, BM-  
174 MSCs demonstrated strong positive expression for CD44, CD73, CD90, and CD105, while  
175 showing negative expression of CD45, confirming their mesenchymal identity (Figure 1B). In  
176 contrast, PBMCs, composed of a heterogeneous cell type, generally express all markers, with  
177 CD44 and CD45 being universally expressed across all cells (Figure 1B). Immunocytochemistry  
178 further revealed that BM-MSCs were negative for CD45 and positive for CD73 and CD105, which  
179 is consistent with the results observed for BMACs, whereas PBMCs showed all-positive  
180 expression for CD45, while the expression of CD73 and CD105 was barely detected (Figure 1C).  
181 These findings indicate that porcine BM-MSCs maintain a distinct MSC marker expression, which  
182 clearly differentiates them from PBMCs.

183

#### 184 **Comparative analysis of gene expression in BM-MSCs and BMACs**

185 To analyze the differential gene expression patterns among porcine BMACs, BM-MSCs, and  
186 PBMCs, we performed a comprehensive gene expression analysis using mRNA-Seq data. The  
187 DEGs between BMACs and PBMCs and between BM-MSCs and PBMCs were compared (Figure  
188 2A). As shown on the Venn diagram, 1,297 upregulated and 1,399 downregulated genes were  
189 observed in the comparison between BMACs and PBMCs, whereas 1,873 upregulated and 2,062  
190 downregulated genes were observed in the comparison between BM-MSCs and PBMCs. The  
191 overlap included 4,467 upregulated and 4,798 downregulated genes, with 365 contra-regulated  
192 genes shared between comparisons.

193 Gene expression profiles were visualized using a clustering heatmap (Figure 2B), which showed  
194 the hierarchical clustering of gene expression profiles across PBMCs, PK(15) cells, BMACs, and  
195 BM-MSCs. The clustering revealed distinct gene expression profiles, highlighting the unique  
196 regulatory mechanisms of each cell type. These results indicate that BM-MSCs exhibit a different

197 expression pattern from that of PBMCs but a significantly similar expression pattern to that of  
198 BMACs.

199

### 200 **Gene ontology (GO) enrichment analysis of BM-MSCs**

201 To identify significant biological pathways associated with BM-MSCs, GO enrichment analysis  
202 of DEGs was performed using the Ingenuity Pathway Analysis (IPA) software. In this analysis,  
203 DEGs were subjected to pathway enrichment analysis to identify significant changes in BM-MSCs  
204 compared with those in PBMCs and BMACs. The statistical significance (*p*-value) of each  
205 pathway was determined, and pathways with a *p*-value of  $\leq 0.05$  were considered significant.

206 The significant pathways identified by GO analysis are shown in Figure 3. The gene enrichment  
207 assay revealed the most enriched pathways, with each bubble representing one pathway (Figure  
208 3A). The size and color of the bubble indicate the fold enrichment and significance level,  
209 respectively. The key pathways identified were cytokine-cytokine receptor interaction, allograft  
210 rejection, rheumatoid arthritis, inflammatory bowel disease, and the intestinal immune network for  
211 IgA production. Furthermore, as shown in Figure 3B, the pathway enrichment bar plot shows the  
212 number of upregulated (red) and downregulated (green) genes for each significantly enriched  
213 pathway, with the blue line indicating the *p*-value. This plot further shows the significant pathways  
214 identified in the pathway enrichment bubble plot.

215

### 216 **Pathway enrichment and network analysis revealed that porcine BM-MSCs are closely** 217 **related to immune regulation**

218 Using IPA, we performed a pathway enrichment analysis of DEGs identified in porcine BM-MSCs  
219 compared with those in PBMCs. This analysis revealed several key canonical pathways, with  
220 significant *z*-scores indicating either activation or inhibition. The top biological functions were the

221 pulmonary fibrosis idiopathic signaling pathway, hepatic fibrosis/hepatic stellate cell activation,  
222 hepatic fibrosis signaling pathway, extracellular matrix organization, and the pathogen-induced  
223 cytokine storm signaling pathway (Figure 4A). The network analysis of DEGs in porcine BM-  
224 MSCs revealed the central role of the transforming growth factor-beta (TGF- $\beta$ ) signaling pathway,  
225 linking key downstream pathways involved in cellular differentiation, fibrosis, and immune  
226 response modulation (Figure 4B). Furthermore, the biological network of TGF- $\beta$  as an upstream  
227 regulator in the subcellular environment indicates the extensive regulatory influence of TGF- $\beta$  on  
228 a wide array of genes associated with tissue repair, immune modulation, and cellular homeostasis  
229 (Figure 4C). These findings collectively emphasize the intricate signaling networks active in BM-  
230 MSCs, highlighting the significant role of TGF- $\beta$  in immune regulation.

231

### 232 **Immunomodulatory effects of BM-MSCs in xenogeneic status**

233 Our data revealed that BM-MSCs exhibited higher TGF- $\beta$  expression levels than PBMCs. To  
234 evaluate the immunomodulatory effects of BM-MSCs under xenogeneic conditions, PMA-  
235 differentiated THP-1 cells, treated with 1  $\mu$ g/mL LPS for 24 h, were indirectly co-cultured with  
236 BM-MSCs using a Transwell system. The expression levels of key cytokines and markers  
237 associated with inflammation were also assessed. The results revealed a significant decrease in the  
238 expression of pro-inflammatory cytokines, IL-6 and TNF $\alpha$ , in PMA-differentiated THP-1 cells  
239 treated with LPS and co-cultured with BM-MSCs (BM-MSC group) compared with the LPS group  
240 (Figures 5A and B). In contrast, the anti-inflammatory cytokine IL-10 was significantly  
241 upregulated in the BM-MSC group, and its mRNA levels were maintained (Figure 5C). In addition,  
242 significant downregulation of the expression of CCR7, a marker associated with the M1  
243 macrophage phenotype, and slight upregulation of the expression of CD163, a marker for the M2  
244 macrophage phenotype, were observed in the BM-MSC group compared with the WT group

245 (Figures 5D and E). These findings suggest that BM-MSCs exert a potent immunomodulatory  
246 effect by suppressing pro-inflammatory responses and promoting an anti-inflammatory M2-like  
247 macrophage phenotype under xenogeneic conditions.

248

249

## DISCUSSION

250 In the present study, we provided a detailed characterization of porcine BM-MSCs and compared  
251 their gene expression profiles and immunomodulatory properties with those of PBMCs and  
252 BMACs. Our findings offer significant insights into the molecular and phenotypic distinctiveness  
253 of BM-MSCs, emphasizing their potential for therapeutic applications in transplantation and  
254 regenerative medicine.

255 A key aspect of the present study was the use of complementary techniques, including qRT-PCR,  
256 flow cytometry, immunocytochemistry, and RNA sequencing. These comprehensive techniques  
257 enabled us to confirm that classical MSC markers, including CD44, CD73, CD90, and CD105,  
258 were expressed in BM-MSCs, whereas the hematopoietic marker, CD45, was not observed. This  
259 expression profile was consistent with the established criteria for MSC identification across  
260 different species, indicating the conserved nature of these markers (6, 42-44). It has been reported  
261 in some studies that CD73 and CD105 are not expressed in porcine BM-MSC, unlike their human  
262 counterparts (45, 46). However, our data confirmed the RNA and protein expression of these  
263 markers in porcine BM-MSCs, aligning them more closely with the characteristics of human BM-  
264 MSCs (47, 48). BMACs are a heterogeneous population of cells, including macrophages, stromal  
265 cells, and other bone marrow-derived cells, that provide a supportive environment for stem cell  
266 function (49, 50). The similarity in gene expression patterns between BM-MSCs and BMACs  
267 suggests that BM-MSCs retain their stem cell characteristics. Furthermore, the distinct expression

268 patterns in BM-MSCs compared with those in PBMCs may enhance their therapeutic potential,  
269 particularly in tissue regeneration and immune modulation (51).

270 Transcriptome profiling revealed significant differences between BM-MSCs and PBMCs, with a  
271 significant number of DEGs observed (Figure 2). This differential expression underscores the  
272 unique regulatory mechanisms inherent in BM-MSCs, which are potentially advantageous for  
273 regulating immune responses (52, 53). Notably, all of the upregulated genes in the top 10 DEGs  
274 are located downstream of the TGF- $\beta$  signaling pathway, a finding further corroborated by the IPA  
275 analysis (Supplementary file 4, Figure 4B and C). These results suggest that the differences in  
276 unique regulatory mechanisms between PBMCs and MSCs are primarily driven by the TGF- $\beta$   
277 pathway. Additionally, the overlap of upregulated and downregulated genes between BM-MSCs  
278 and BMACs suggests that both cell types share common regulatory pathways. GO enrichment  
279 analysis revealed key pathways significantly associated with BM-MSCs, such as cytokine-  
280 cytokine receptor interaction and allograft rejection. These pathways are crucial for modulating  
281 immune responses and promoting tissue repair, thereby highlighting the therapeutic potential of  
282 BM-MSCs for transplantation (54-56).

283 BM-MSCs exhibited higher TGF- $\beta$  levels than PBMCs, indicating their central role in immune  
284 regulation and immunomodulatory functions (4, 57, 58). Our pathway enrichment and network  
285 analyses revealed TGF- $\beta$  signaling as a pivotal node that connects various downstream pathways  
286 involved in fibrosis, cellular differentiation, and immune regulation (Figure 3). This finding is  
287 consistent with those of recent studies, emphasizing the importance of TGF- $\beta$  in maintaining  
288 immune homeostasis and facilitating tissue repair (59, 60). Recent studies also indicate that TGF-  
289  $\beta$ , produced by BM-MSCs, plays a role in influencing the proliferation of CD34<sup>+</sup> cells and  
290 regulating hematopoiesis (61). Furthermore, we observed a reduction in pro-inflammatory  
291 cytokines (IL-6 and TNF $\alpha$ ) and an upregulation of the anti-inflammatory cytokine, IL-10, in the

292 BM-MSC group under xenogeneic conditions (62). Additionally, the expression of CCR7, an M1  
293 macrophage marker, was significantly decreased, while CD163, an M2 macrophage marker, was  
294 increased in the BM-MSC group (63). These results suggest that BM-MSCs regulate immune  
295 responses through downstream signals mediated by TGF- $\beta$ , leading to the polarization of pro-  
296 inflammatory M1 macrophages into anti-inflammatory M2 macrophages under both allo-reactive  
297 and xenogeneic conditions.

298 These results are promising; however, certain challenges must be addressed before BM-MSCs can  
299 be widely applied in clinical settings. One significant issue is the long-term safety and efficacy of  
300 BM-MSC-based therapies, particularly in xenogeneic contexts where immune rejection remains a  
301 major concern (20). TGF- $\beta$  is an immunoregulatory cytokine that plays a crucial role in the  
302 differentiation of Th9, Th17, and regulatory T cells, and its influence has been extensively studied  
303 in both acute and chronic responses in allogeneic transplantation (64). Also, TGF- $\beta$  acts on  
304 macrophages to induce an anti-inflammatory response via the Smad2/3 pathway and promotes  
305 M2-like macrophage polarization (65, 66). A previous study has shown that BM-MSCs secreting  
306 TGF- $\beta$ , when administered to septic mice, significantly reduced inflammatory macrophages,  
307 suggesting that TGF- $\beta$  can regulate immune responses, at least during the acute phase (67).  
308 Although our findings were obtained under xenogeneic conditions and in vitro, they exhibit a  
309 similar pattern (Figure 5). Furthermore, the higher levels of TGF- $\beta$  expression in BM-MSCs and  
310 their capacity to induce an anti-inflammatory macrophage response indicate their potential to  
311 reduce graft rejection and improve transplant outcomes (68, 69). However, further research is  
312 necessary to fully elucidate the mechanisms through which BM-MSCs exert these effects,  
313 particularly in long-term studies, and to assess the efficacy and safety of BM-MSC-based therapies  
314 in clinical settings.

315 In conclusion, our study provides a comprehensive profile of porcine BM-MSCs and describes  
316 their distinct molecular characteristics and immunomodulatory potential. Our findings support the  
317 ongoing investigation of BM-MSCs in the context of xenotransplantation and regenerative  
318 medicine with the aim of developing novel therapies that can effectively manage immune  
319 responses and enhance tissue regeneration.

320

### 321 **Resource availability**

322 Lead contact: Further information and requests for resources and reagents should be directed to and  
323 will be fulfilled by the lead contact, Jeong Ho Hwang (jeongho.hwang@kitox.re.kr).

324 Materials availability: This study did not generate any unique reagents.

325

### 326 **Acknowledgments**

327 The author(s) disclosed receipt of the following financial support for the research, authorship,  
328 and/or publication of this article: This work was supported by the grants from Korea institute of  
329 Toxicology (KIT, Korea) and the Ministry of Science and ICT (grant numbers KK-2408-01,  
330 1711195889).

331

332



## 333 **References**

- 334 1. ~~1.1.~~ Ullah I, Subbarao RB, Rho GJ. Human mesenchymal stem cells - current trends  
335 and future prospective. *Biosci Rep.* 2015;35(2). <https://doi.org/10.1042/BSR20150025>
- 336 2. Squillaro T, Peluso G, Galderisi U. Clinical Trials With Mesenchymal Stem Cells: An Update.  
337 *Cell Transplant.* 2016;25(5):829-48. <https://doi.org/10.3727/096368915X689622>
- 338 3. Zhang Y, Ravikumar M, Ling L, Nurcombe V, Cool SM. Age-Related Changes in the  
339 Inflammatory Status of Human Mesenchymal Stem Cells: Implications for Cell Therapy.  
340 *Stem Cell Reports.* 2021;16(4):694-707. <https://doi.org/10.1016/j.stemcr.2021.01.021>
- 341 4. Trounson A, McDonald C. Stem Cell Therapies in Clinical Trials: Progress and Challenges.  
342 *Cell Stem Cell.* 2015;17(1):11-22. <https://doi.org/10.1016/j.stem.2015.06.007>
- 343 5. Liu P, An Y, Zhu T, Tang S, Huang X, Li S, et al. Mesenchymal stem cells: Emerging concepts  
344 and recent advances in their roles in organismal homeostasis and therapy. *Front Cell Infect*  
345 *Microbiol.* 2023;13:1131218. <https://doi.org/10.3389/fcimb.2023.1131218>
- 346 6. Zimmermann CE, Mackens-Kiani L, Acil Y, Terheyden H. Characterization of porcine  
347 mesenchymal stromal cells and their proliferative and osteogenic potential in long-term  
348 culture. *J Stem Cells Regen Med.* 2021;17(2):49-55. <https://doi.org/10.46582/jsrm.1702008>
- 349 7. Kounng Ngeun S, Shimizu M, Kaneda M. Characterization of Rabbit Mesenchymal  
350 Stem/Stromal Cells after Cryopreservation. *Biology (Basel).* 2023;12(10).  
351 <https://doi.org/10.3390/biology12101312>
- 352 8. Ghaneialvar H, Soltani L, Rahmani HR, Lotfi AS, Soleimani M. Characterization and  
353 Classification of Mesenchymal Stem Cells in Several Species Using Surface Markers for Cell  
354 Therapy Purposes. *Indian J Clin Biochem.* 2018;33(1):46-52. <https://doi.org/10.1007/s12291-017-0641-x>
- 356 9. Rashid U, Yousaf A, Yaqoob M, Saba E, Moaen-Ud-Din M, Waseem S, et al.  
357 Characterization and differentiation potential of mesenchymal stem cells isolated from  
358 multiple canine adipose tissue sources. *BMC Vet Res.* 2021;17(1):388.  
359 <https://doi.org/10.1186/s12917-021-03100-8>
- 360 10. Dias IE, Pinto PO, Barros LC, Viegas CA, Dias IR, Carvalho PP. Mesenchymal stem cells  
361 therapy in companion animals: useful for immune-mediated diseases? *BMC Vet Res.*  
362 2019;15(1):358. <https://doi.org/10.1186/s12917-019-2087-2>

- 363 11. Prządka P, Buczak K, Frejlich E, Gasior L, Suliga K, Kielbowicz Z. The Role of  
364 Mesenchymal Stem Cells (MSCs) in Veterinary Medicine and Their Use in Musculoskeletal  
365 Disorders. *Biomolecules*. 2021;11(8). <https://doi.org/10.3390/biom11081141>
- 366 12. Picazo RA, Rojo C, Rodriguez-Quiros J, Gonzalez-Gil A. Current Advances in Mesenchymal  
367 Stem Cell Therapies Applied to Wounds and Skin, Eye, and Neuromuscular Diseases in  
368 Companion Animals. *Animals (Basel)*. 2024;14(9). <https://doi.org/10.3390/ani14091363>
- 369 13. Patterson JK, Lei XG, Miller DD. The pig as an experimental model for elucidating the  
370 mechanisms governing dietary influence on mineral absorption. *Exp Biol Med (Maywood)*.  
371 2008;233(6):651-64. <https://doi.org/10.3181/0709-MR-262>
- 372 14. Lunney JK, Van Goor A, Walker KE, Hailstock T, Franklin J, Dai C. Importance of the pig as  
373 a human biomedical model. *Sci Transl Med*. 2021;13(621):eabd5758.  
374 <https://doi.org/10.1126/scitranslmed.abd5758>
- 375 15. Li J, Zhao T, Guan D, Pan Z, Bai Z, Teng J, et al. Learning functional conservation between  
376 human and pig to decipher evolutionary mechanisms underlying gene expression and  
377 complex traits. *Cell Genom*. 2023;3(10):100390. <https://doi.org/10.1016/j.xgen.2023.100390>
- 378 16. Giraud S, Favreau F, Chatauret N, Thuillier R, Maiga S, Hauet T. Contribution of large pig  
379 for renal ischemia-reperfusion and transplantation studies: the preclinical model. *J Biomed*  
380 *Biotechnol*. 2011;2011:532127. <https://doi.org/10.1155/2011/532127>
- 381 17. Lelovas PP, Kostomitsopoulos NG, Xanthos TT. A comparative anatomic and physiologic  
382 overview of the porcine heart. *J Am Assoc Lab Anim Sci*. 2014;53(5):432-8.
- 383 18. Moazami N, Stern JM, Khalil K, Kim JI, Narula N, Mangiola M, et al. Pig-to-human heart  
384 xenotransplantation in two recently deceased human recipients. *Nat Med*. 2023;29(8):1989-  
385 97. <https://doi.org/10.1038/s41591-023-02471-9>
- 386 19. Wang Y, Chen G, Pan D, Guo H, Jiang H, Wang J, et al. Pig-to-human kidney xenotransplants  
387 using genetically modified minipigs. *Cell Rep Med*. 2024;5(10):101744.  
388 <https://doi.org/10.1016/j.xcrm.2024.101744>
- 389 20. Li J, Ezzelarab MB, Cooper DK. Do mesenchymal stem cells function across species barriers?  
390 Relevance for xenotransplantation. *Xenotransplantation*. 2012;19(5):273-85.  
391 <https://doi.org/10.1111/xen.12000>
- 392 21. Bharti D, Shivakumar SB, Subbarao RB, Rho GJ. Research Advancements in Porcine  
393 Derived Mesenchymal Stem Cells. *Curr Stem Cell Res Ther*. 2016;11(1):78-93.

- 394 <https://doi.org/10.2174/1574888x10666150723145911>
- 395 22. Huang Y, Wu Q, Tam PKH. Immunomodulatory Mechanisms of Mesenchymal Stem Cells  
396 and Their Potential Clinical Applications. *Int J Mol Sci.* 2022;23(17).  
397 <https://doi.org/10.3390/ijms231710023>
- 398 23. Deo D, Marchioni M, Rao P. Mesenchymal Stem/Stromal Cells in Organ Transplantation.  
399 *Pharmaceutics.* 2022;14(4). <https://doi.org/10.3390/pharmaceutics14040791>
- 400 24. Ben Menachem-Zidon O, Gropp M, Reubinoff B, Shveiky D. Mesenchymal stem cell  
401 transplantation improves biomechanical properties of vaginal tissue following full-thickness  
402 incision in aged rats. *Stem Cell Reports.* 2022;17(11):2565-78.  
403 <https://doi.org/10.1016/j.stemcr.2022.09.005>
- 404 25. Li Q, Lan P. Activation of immune signals during organ transplantation. *Signal Transduct*  
405 *Target Ther.* 2023;8(1):110. <https://doi.org/10.1038/s41392-023-01377-9>
- 406 26. Han Y, Yang J, Fang J, Zhou Y, Candi E, Wang J, et al. The secretion profile of mesenchymal  
407 stem cells and potential applications in treating human diseases. *Signal Transduct Target Ther.*  
408 2022;7(1):92. <https://doi.org/10.1038/s41392-022-00932-0>
- 409 27. Mclau K, Hambright WS, Huard J, Stoddart MJ, Bahney CS. Cellular expansion of MSCs:  
410 Shifting the regenerative potential. *Aging Cell.* 2023;22(1):e13759.  
411 <https://doi.org/10.1111/accel.13759>
- 412 28. Li P, Ou Q, Shi S, Shao C. Immunomodulatory properties of mesenchymal stem cells/dental  
413 stem cells and their therapeutic applications. *Cell Mol Immunol.* 2023;20(6):558-69.  
414 <https://doi.org/10.1038/s41423-023-00998-y>
- 415 29. Lam ATL, Reuveny S, Oh SK. Human mesenchymal stem cell therapy for cartilage repair:  
416 Review on isolation, expansion, and constructs. *Stem Cell Res.* 2020;44:101738.  
417 <https://doi.org/10.1016/j.scr.2020.101738>
- 418 30. Dominici M, Le Blanc K, Mueller I, Slaper-Cortenbach I, Marini F, Krause D, et al. Minimal  
419 criteria for defining multipotent mesenchymal stromal cells. The International Society for  
420 Cellular Therapy position statement. *Cytotherapy.* 2006;8(4):315-7.  
421 <https://doi.org/10.1080/14653240600855905>
- 422 31. Groth A, Ottinger S, Kleist C, Mohr E, Golriz M, Schultze D, et al. Evaluation of porcine  
423 mesenchymal stem cells for therapeutic use in human liver cancer. *Int J Oncol.*  
424 2012;40(2):391-401. <https://doi.org/10.3892/ijo.2011.1217>

- 425 32. Galow AM, Goldammer T, Hoeflich A. Xenogeneic and Stem Cell-Based Therapy for  
426 Cardiovascular Diseases: Genetic Engineering of Porcine Cells and Their Applications in  
427 Heart Regeneration. *Int J Mol Sci.* 2020;21(24). <https://doi.org/10.3390/ijms21249686>
- 428 33. Caplan AI. Mesenchymal Stem Cells: Time to Change the Name! *Stem Cells Transl Med.*  
429 2017;6(6):1445-51. <https://doi.org/10.1002/sctm.17-0051>
- 430 34. Podesta MA, Remuzzi G, Casiraghi F. Mesenchymal Stromal Cells for Transplant Tolerance.  
431 *Front Immunol.* 2019;10:1287. <https://doi.org/10.3389/fimmu.2019.01287>
- 432 35. Mou L, Wang TB, Wang X, Pu Z. Advancing diabetes treatment: the role of mesenchymal  
433 stem cells in islet transplantation. *Front Immunol.* 2024;15:1389134.  
434 <https://doi.org/10.3389/fimmu.2024.1389134>
- 435 36. Crippa S, Bernardo ME. Mesenchymal Stromal Cells: Role in the BM Niche and in the  
436 Support of Hematopoietic Stem Cell Transplantation. *Hemasphere.* 2018;2(6):e151.  
437 <https://doi.org/10.1097/HS9.0000000000000151>
- 438 37. Benova A, Tencerova M. Obesity-Induced Changes in Bone Marrow Homeostasis. *Front*  
439 *Endocrinol (Lausanne).* 2020;11:294. <https://doi.org/10.3389/fendo.2020.00294>
- 440 38. Chao YH, Lin CW, Pan HH, Yang SF, Weng TF, Peng CT, et al. Increased apoptosis and  
441 peripheral blood mononuclear cell suppression of bone marrow mesenchymal stem cells in  
442 severe aplastic anemia. *Pediatr Blood Cancer.* 2018;65(9):e27247.  
443 <https://doi.org/10.1002/pbc.27247>
- 444 39. Xiong H, Guo Z, Tang Z, Ai X, Qi Q, Liu X, et al. Mesenchymal Stem Cells Activate the  
445 MEK/ERK Signaling Pathway and Enhance DNA Methylation via DNMT1 in PBMC from  
446 Systemic Lupus Erythematosus. *Biomed Res Int.* 2020;2020:4174082.  
447 <https://doi.org/10.1155/2020/4174082>
- 448 40. Sherman BT, Hao M, Qiu J, Jiao X, Baseler MW, Lane HC, et al. DAVID: a web server for  
449 functional enrichment analysis and functional annotation of gene lists (2021 update). *Nucleic*  
450 *Acids Res.* 2022;50(W1):W216-W21. <https://doi.org/10.1093/nar/gkac194>
- 451 41. Huang da W, Sherman BT, Lempicki RA. Systematic and integrative analysis of large gene  
452 lists using DAVID bioinformatics resources. *Nat Protoc.* 2009;4(1):44-57.  
453 <https://doi.org/10.1038/nprot.2008.211>
- 454 42. Wang X, Zheng F, Liu O, Zheng S, Liu Y, Wang Y, et al. Epidermal growth factor can optimize  
455 a serum-free culture system for bone marrow stem cell proliferation in a miniature pig model.

- 456 In Vitro Cell Dev Biol Anim. 2013;49(10):815-25. [https://doi.org/10.1007/s11626-013-9665-](https://doi.org/10.1007/s11626-013-9665-6)  
457 6
- 458 43. Juhasova J, Juhas S, Klima J, Strnad J, Holubova M, Motlik J. Osteogenic differentiation  
459 of miniature pig mesenchymal stem cells in 2D and 3D environment. *Physiol Res.*  
460 2011;60(3):559-71. <https://doi.org/10.33549/physiolres.932028>
- 461 44. Bruckner S, Tautenhahn HM, Winkler S, Stock P, Dollinger M, Christ B. A fat option for the  
462 pig: hepatocytic differentiated mesenchymal stem cells for translational research. *Exp Cell*  
463 *Res.* 2014;321(2):267-75. <https://doi.org/10.1016/j.yexcr.2013.10.018>
- 464 45. Schweizer R, Waldner M, Oksuz S, Zhang W, Komatsu C, Plock JA, et al. Evaluation of  
465 Porcine Versus Human Mesenchymal Stromal Cells From Three Distinct Donor Locations  
466 for Cytotherapy. *Front Immunol.* 2020;11:826. <https://doi.org/10.3389/fimmu.2020.00826>
- 467 46. Noort WA, Oerlemans MI, Rozemuller H, Feyen D, Jaksani S, Stecher D, et al. Human versus  
468 porcine mesenchymal stromal cells: phenotype, differentiation potential, immunomodulation  
469 and cardiac improvement after transplantation. *J Cell Mol Med.* 2012;16(8):1827-39.  
470 <https://doi.org/10.1111/j.1582-4934.2011.01455.x>
- 471 47. Su J, Chen X, Huang Y, Li W, Li J, Cao K, et al. Phylogenetic distinction of iNOS and IDO  
472 function in mesenchymal stem cell-mediated immunosuppression in mammalian species. *Cell*  
473 *Death Differ.* 2014;21(3):388-96. <https://doi.org/10.1038/cdd.2013.149>
- 474 48. Khaveh N, Buschow R, Metzger J. Deciphering transcriptome patterns in porcine  
475 mesenchymal stem cells promoting phenotypic maintenance and differentiation by key driver  
476 genes. *Front Cell Dev Biol.* 2024;12:1478757. <https://doi.org/10.3389/fcell.2024.1478757>
- 477 49. Wang J, Dai X, Hsu C, Ming C, He Y, Zhang J, et al. Discrimination of the heterogeneity of  
478 bone marrow-derived dendritic cells. *Mol Med Rep.* 2017;16(5):6787-93.  
479 <https://doi.org/10.3892/mmr.2017.7448>
- 480 50. Inaba K, Inaba M, Romani N, Aya H, Deguchi M, Ikehara S, et al. Generation of large  
481 numbers of dendritic cells from mouse bone marrow cultures supplemented with  
482 granulocyte/macrophage colony-stimulating factor. *J Exp Med.* 1992;176(6):1693-702.  
483 <https://doi.org/10.1084/jem.176.6.1693>
- 484 51. Salem HK, Thiemermann C. Mesenchymal stromal cells: current understanding and clinical  
485 status. *Stem Cells.* 2010;28(3):585-96. <https://doi.org/10.1002/stem.269>
- 486 52. Rossello-Gelabert M, Gonzalez-Pujana A, Igartua M, Santos-Vizcaino E, Hernandez RM.

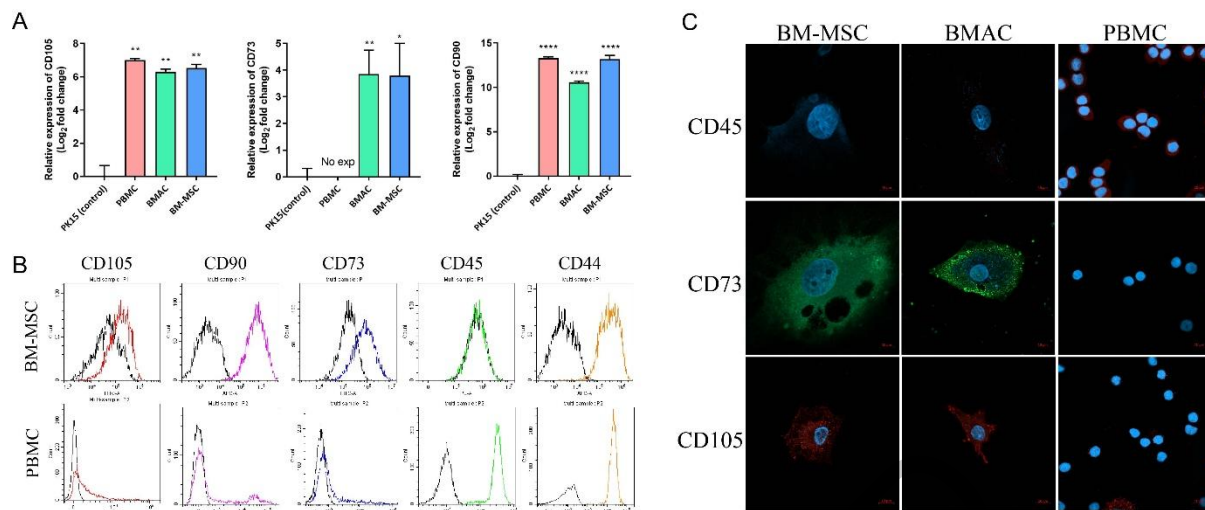
- 487 Clinical progress in MSC-based therapies for the management of severe COVID-19.  
488 Cytokine Growth Factor Rev. 2022;68:25-36. <https://doi.org/10.1016/j.cytogfr.2022.07.002>
- 489 53. Jovic D, Yu Y, Wang D, Wang K, Li H, Xu F, et al. A Brief Overview of Global Trends in  
490 MSC-Based Cell Therapy. Stem Cell Rev Rep. 2022;18(5):1525-45.  
491 <https://doi.org/10.1007/s12015-022-10369-1>
- 492 54. Kurtzberg J, Abdel-Azim H, Carpenter P, Chaudhury S, Horn B, Mahadeo K, et al. A Phase  
493 3, Single-Arm, Prospective Study of Remestemcel-L, Ex Vivo Culture-Expanded Adult  
494 Human Mesenchymal Stromal Cells for the Treatment of Pediatric Patients Who Failed to  
495 Respond to Steroid Treatment for Acute Graft-versus-Host Disease. Biol Blood Marrow  
496 Transplant. 2020;26(5):845-54. <https://doi.org/10.1016/j.bbmt.2020.01.018>
- 497 55. Azizi Z, Abbaszadeh R, Sahebnasagh R, Norouzy A, Motevaseli E, Maedler K. Bone marrow  
498 mesenchymal stromal cells for diabetes therapy: touch, fuse, and fix? Stem Cell Res Ther.  
499 2022;13(1):348. <https://doi.org/10.1186/s13287-022-03028-2>
- 500 56. Zhang R, Yu J, Zhang N, Li W, Wang J, Cai G, et al. Bone marrow mesenchymal stem cells  
501 transfer in patients with ST-segment elevation myocardial infarction: single-blind,  
502 multicenter, randomized controlled trial. Stem Cell Res Ther. 2021;12(1):33.  
503 <https://doi.org/10.1186/s13287-020-02096-6>
- 504 57. Xu C, Yu P, Han X, Du L, Gan J, Wang Y, et al. TGF-beta promotes immune responses in the  
505 presence of mesenchymal stem cells. J Immunol. 2014;192(1):103-9.  
506 <https://doi.org/10.4049/jimmunol.1302164>
- 507 58. Li R, Wang R, Zhong S, Asghar F, Li T, Zhu L, et al. TGF-beta1-overexpressing mesenchymal  
508 stem cells reciprocally regulate Th17/Treg cells by regulating the expression of IFN-gamma.  
509 Open Life Sci. 2021;16(1):1193-202. <https://doi.org/10.1515/biol-2021-0118>
- 510 59. Battle E, Massague J. Transforming Growth Factor-beta Signaling in Immunity and Cancer.  
511 Immunity. 2019;50(4):924-40. <https://doi.org/10.1016/j.immuni.2019.03.024>
- 512 60. Ramirez H, Patel SB, Pastar I. The Role of TGFbeta Signaling in Wound Epithelialization.  
513 Adv Wound Care (New Rochelle). 2014;3(7):482-91.  
514 <https://doi.org/10.1089/wound.2013.0466>
- 515 61. Kawamura H, Nakatsuka R, Matsuoka Y, Sumide K, Fujioka T, Asano H, et al. TGF-beta  
516 Signaling Accelerates Senescence of Human Bone-Derived CD271 and SSEA-4 Double-  
517 Positive Mesenchymal Stromal Cells. Stem Cell Reports. 2018;10(3):920-32.  
518 <https://doi.org/10.1016/j.stemcr.2018.01.030>

- 519 62. Maggini J, Mirkin G, Bognanni I, Holmberg J, Piazzon IM, Nepomnaschy I, et al. Mouse  
520 bone marrow-derived mesenchymal stromal cells turn activated macrophages into a  
521 regulatory-like profile. *PLoS One.* 2010;5(2):e9252.  
522 <https://doi.org/10.1371/journal.pone.0009252>
- 523 63. Fu SP, Wu XC, Yang RL, Zhao DZ, Cheng J, Qian H, et al. The role and mechanisms of  
524 mesenchymal stem cells regulating macrophage plasticity in spinal cord injury. *Biomed*  
525 *Pharmacother.* 2023;168:115632. <https://doi.org/10.1016/j.biopha.2023.115632>
- 526 64. Iwashima M, Love R. Potential of targeting TGF-beta for organ transplant patients. *Future*  
527 *Med Chem.* 2013;5(3):281-9. <https://doi.org/10.4155/fmc.12.215>
- 528 65. Zhang F, Wang H, Wang X, Jiang G, Liu H, Zhang G, et al. TGF-beta induces M2-like  
529 macrophage polarization via SNAIL-mediated suppression of a pro-inflammatory phenotype.  
530 *Oncotarget.* 2016;7(32):52294-306. <https://doi.org/10.18632/oncotarget.10561>
- 531 66. Gauthier T, Yao C, Dowdy T, Jin W, Lim YJ, Patino LC, et al. TGF-beta uncouples glycolysis  
532 and inflammation in macrophages and controls survival during sepsis. *Sci Signal.*  
533 2023;16(797):eade0385. <https://doi.org/10.1126/scisignal.ade0385>
- 534 67. Liu F, Xie J, Zhang X, Wu Z, Zhang S, Xue M, et al. Overexpressing TGF-beta1 in  
535 mesenchymal stem cells attenuates organ dysfunction during CLP-induced septic mice by  
536 reducing macrophage-driven inflammation. *Stem Cell Res Ther.* 2020;11(1):378.  
537 <https://doi.org/10.1186/s13287-020-01894-2>
- 538 68. Wang J, Ding H, Zhou J, Xia S, Shi X, Ren H. Transplantation of Mesenchymal Stem Cells  
539 Attenuates Acute Liver Failure in Mice via an Interleukin-4-dependent Switch to the M2  
540 Macrophage Anti-inflammatory Phenotype. *J Clin Transl Hepatol.* 2022;10(4):669-79.  
541 <https://doi.org/10.14218/JCTH.2021.00127>
- 542 69. Liu F, Xie J, Zhang X, Wu Z, Zhang S, Xue M, et al. Correction: Overexpressing TGF-beta1  
543 in mesenchymal stem cells attenuates organ dysfunction during CLP-induced septic mice by  
544 reducing macrophage-driven. *Stem Cell Res Ther.* 2022;13(1):362.  
545 <https://doi.org/10.1186/s13287-022-03078-6>

546

547

## FIGURE LEGENDS

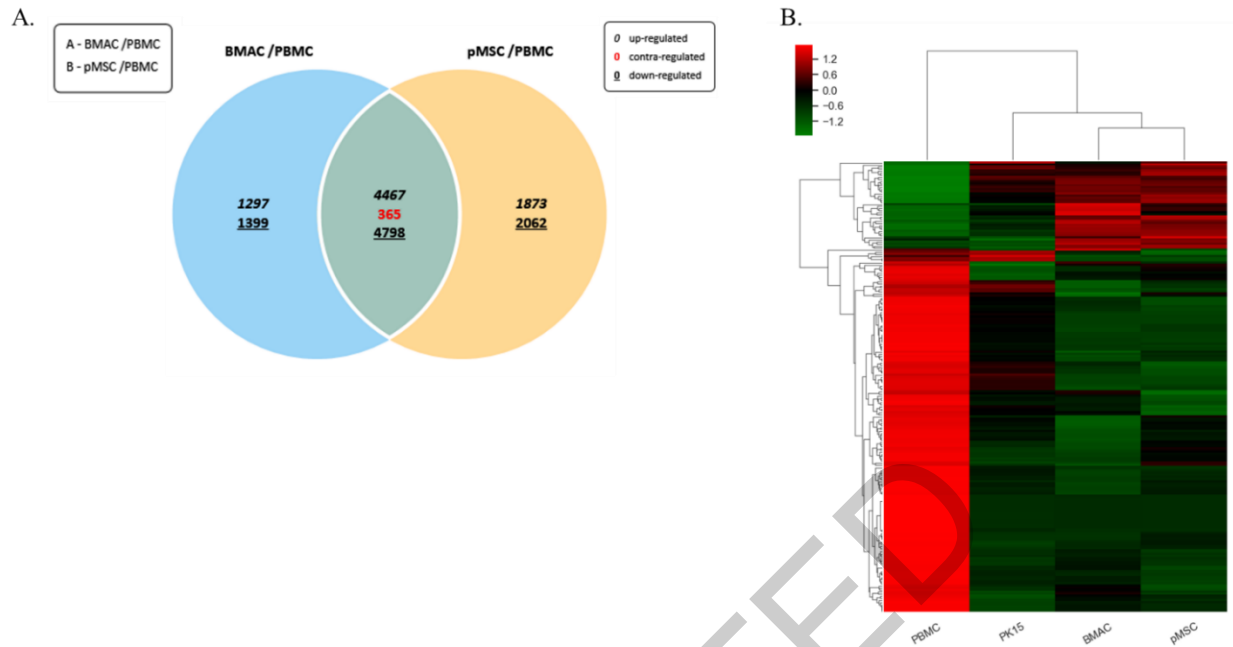
549  
550551 **Figure 1. Characterization of BM-MSCs and BMACs.**

552 Analysis of MSCs marker expression in BM-MSCs and BMACs. (A) mRNA expression levels of  
 553 CD73, CD90, and CD105 were analyzed using qPCR. Mean values represent the mean  $\pm$  standard  
 554 deviation of three independent experiments (\*  $p \leq 0.05$ , \*\*  $p \leq 0.01$ , \*\*\*\*  $p \leq 0.0001$ ). (B)  
 555 Expression levels of CD105, CD90, CD73, CD45, or CD44 were analyzed using flow cytometry.  
 556 Black: No stain control; Color: represented surface molecules. (C) Cells were stained with CD45,  
 557 CD73, or CD105, and nuclei were counter-stained with DAPI. Scale bars, 10  $\mu$ m.

558

559





561  
562

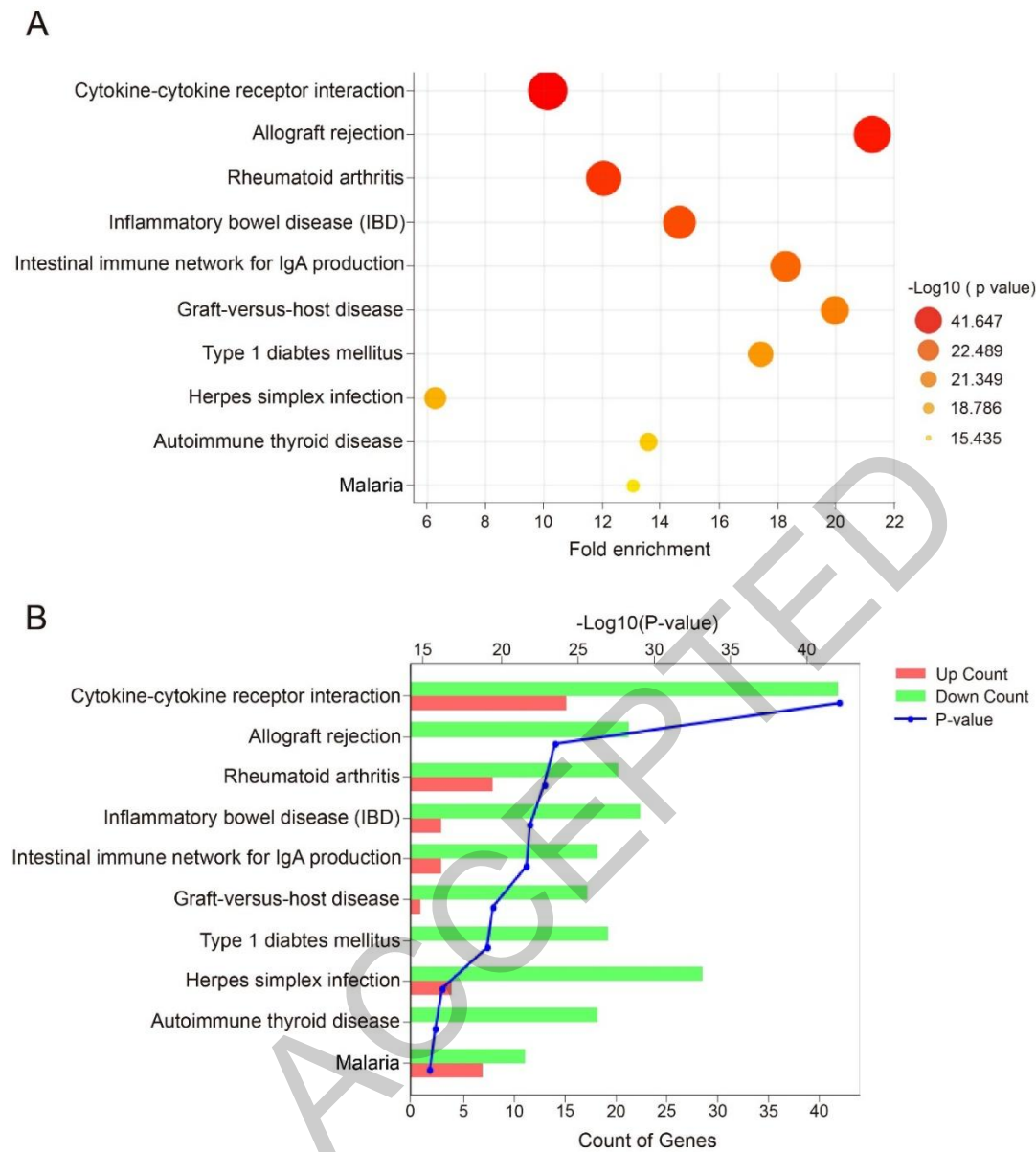
563 **Figure 2. Distribution of comparable expressed genes between BMACs and BM-MSCs.**

564 (A) Venn diagram showing the expression pattern in BMACs and BM-MSCs compared with that  
565 in PBMCs. (B) Clustering heatmap based on the differentially expressed genes.

566

567

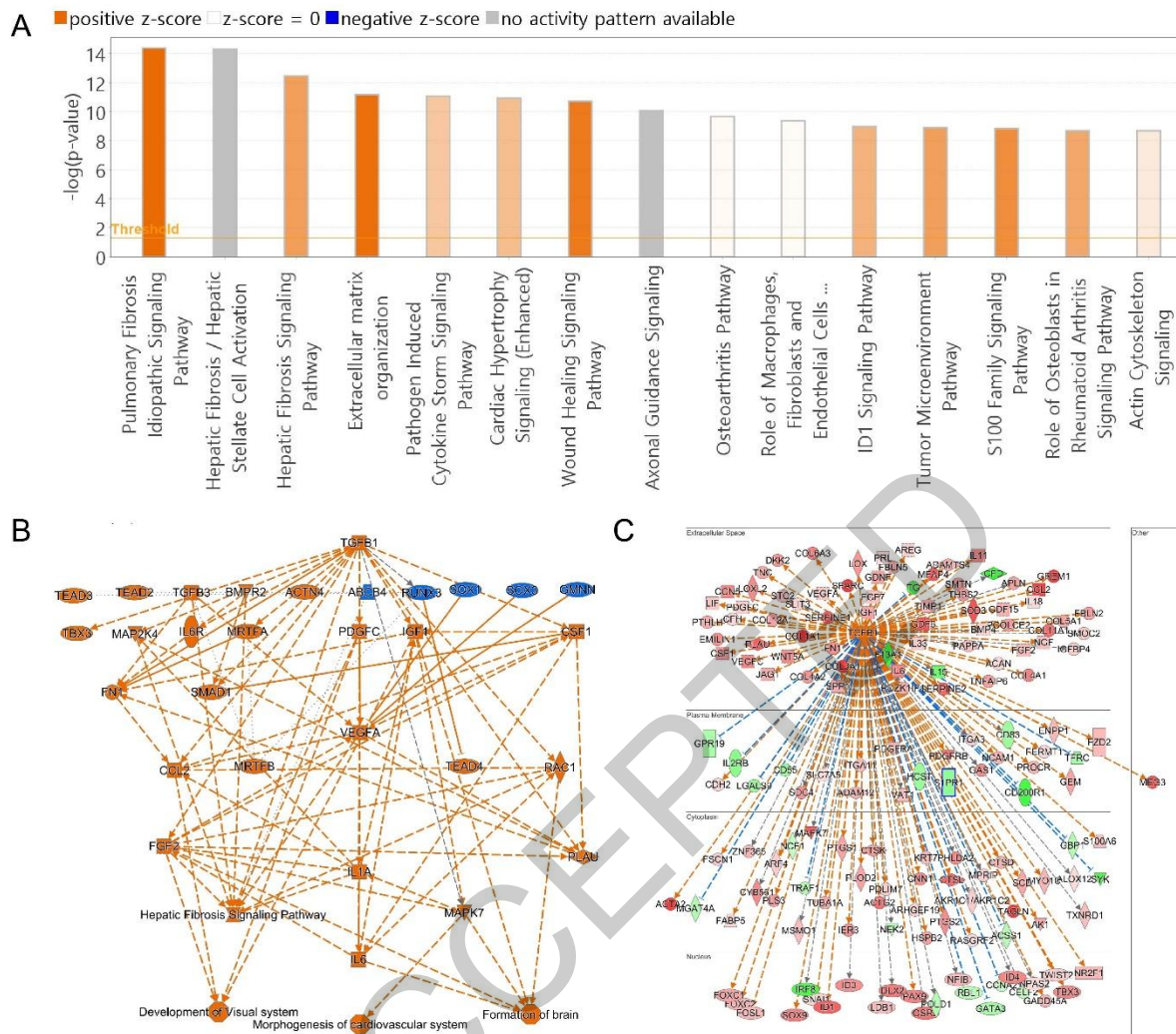
568

570  
571

572 **Figure 3. Enriched Gene Ontology analysis of differentially expressed genes of BM-MSCs.**

573 (A) The most significantly enriched pathways of DEGs obtained from the analysis of RNA-Seq  
 574 data, with the  $p$ -value cutoff indicated as 0.05. Bubble size represents the number of genes enriched  
 575 in a pathway. (B) The top 10 significantly enriched KEGG pathways of DEGs associated with  
 576 MSC regulation, with the  $p$ -value cutoff indicated as 0.05.

577



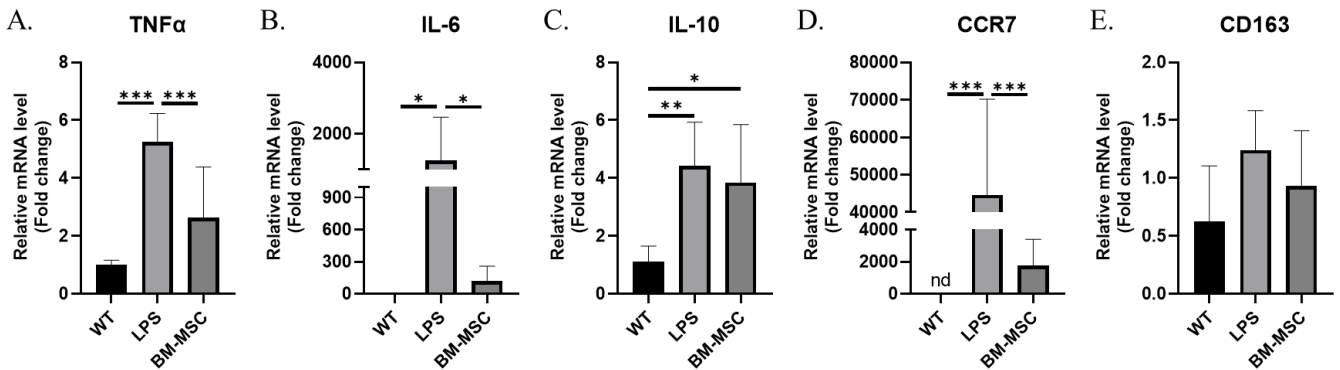
579  
580

581 **Figure 4. Functional characterization of BM-MSCs identified using IPA.**

582 (A) Bar chart showing the most significantly enriched canonical pathways identified from  
 583 differentially expressed genes in porcine BM-MSCs compared with those in PBMCs based on  
 584 RNA-Seq data analysis, with p-value cutoff indicated as 0.05. (B) Graphical summary of RNA-  
 585 Seq data and (C) biological network of TGF-β as an upstream regulator in the subcellular  
 586 environment were analyzed using the IPA software.

587

588

590  
591

592 **Figure 5. mRNA expression levels in PMA-differentiated THP-1 cells co-cultured with BM-**  
593 **MSCs**

594 PMA-differentiated THP-1 cells were treated with 1  $\mu\text{g}/\text{mL}$  LPS for 24 h. mRNA expression levels  
595 of (A) TNF $\alpha$ , (B) IL-6, (C) IL-10, (D) CCR7, and CD163 were analyzed using qPCR. Mean values  
596 represent the mean  $\pm$ SD of six independent experiments. Statistical significance is indicated as  
597 follows: \*  $p \leq 0.05$ , \*\*  $p \leq 0.01$ , \*\*\*  $p \leq 0.001$ , nd; Not detected.

598

599

## TABLES

601 **Tables 1. Primers used for real-time PCR**

Genes	Species		Sequence (5' to 3')
GAPDH	Porcine	F	ACAGACAGCCGTGTGTTCC
		R	ACCTTCACCATCGTGTCTCA
CD73	Porcine	F	CCATGGCCCTGGGAAATCAT
		R	TACTGCCCTCTGGTACCTC
CD90	Porcine	F	GGCATCGCTCTCTTGCTAAC
		R	GGCAGGTTGGTGGTATTCTC
CD105	Porcine	F	CGCTTCAGCTTCCTCCTCCG
		R	CACCACGGGCTCCCGCTTG
GAPDH	Human	F	CCACTCCTCCACCTTTGAC
		R	ACCCTGTTGCTGTAGCCA
TNF- $\alpha$	Human	F	CCCAGGGACCTCTCTCTAATCA
		R	GCTTGAGGGTTTGCTACAACATG
IL-6	Human	F	AAAGAGGCACTGGCAGAAAA
		R	TTTCACCAGGCAAGTCTCCT
IL-10	Human	F	GCTGTCATCGATTTCTTCCC
		R	TCAAACCTCACTCATGGCTTTGT
CCR7	Human	F	AGTCTTCCAGCTGCCCTACA
		R	TCGTAGGCGATGTTGAGTTG
CD163	Human	F	CCAGTCCCAAACACTGTCCT
		R	CACTCTCTATGCAGGCCACA